

# A Holistic Power Optimization Approach for Microgrid Control Based on Deep Reinforcement Learning

Fulong Yao\*, Wanqing Zhao, Matthew Forshaw, Yang Song

**Abstract**—The global energy landscape is undergoing a transformation towards decarbonization, sustainability, and cost-efficiency. In this transition, microgrid systems integrated with renewable energy sources (RES) and energy storage systems (ESS) have emerged as a crucial component. However, optimizing the operational control of such an integrated energy system lacks a holistic view of multiple environmental, infrastructural and economic considerations, not to mention the need to factor in the uncertainties from both the supply and demand. This paper presents a holistic data-driven power optimization approach based on deep reinforcement learning (DRL) for microgrid control considering the multiple needs of decarbonization, sustainability and cost-efficiency. First, two data-driven control schemes, namely the prediction-based (PB) and prediction-free (PF) schemes, are devised to formulate the control problem within a Markov decision process (MDP). Second, a multivariate objective (reward) function is designed to account for the market profits, carbon emissions, peak load, and battery degradation of the microgrid system. Third, we develop a Double Dueling Deep Q Network (D3QN) architecture to optimize the power flows for real-time energy management and determine charging/discharging strategies of ESS. Finally, extensive simulations are conducted to demonstrate the effectiveness and superiority of the proposed approach through a comparative analysis. The results and analysis also suggest the respective circumstances for using the two control schemes in practical implementations with uncertainties.

**Index Terms**—Microgrid systems, Power optimization, Deep reinforcement learning, Decarbonization, Sustainability, Cost-efficiency

## I. INTRODUCTION

WITH the continuous surge in energy demand and the exacerbation of energy shortages, the microgrid landscape is undergoing a transformative shift towards a more balanced and sustainable paradigm [1]. At present, a microgrid that integrates RES and ESS is playing a crucial role in the energy system transition due to its advantages in security, reliability, and cleanliness [2]. RES such as photovoltaic (PV) and wind turbine (WT) help reduce the microgrid’s dependence on fossil fuels or

the national grid, thereby reducing operational costs and greenhouse gas emissions. This, however, exacerbates the uncertainty and uncontrollability of the integrated energy system [3]. The intermittent RES generation combined with the uncertain power demands (as a result of the changing weather conditions and users’ behaviours) poses a fundamental challenge to the power optimization of a microgrid system involving RES and ESS.

In the last few years, the potential has been identified for control-oriented power optimization to address the above challenge, contributing to a resilient and sustainable energy future [4], [5], [6]. For example, considering the battery lifetime characteristics, Das and Ni [7] devised a dynamic programming approach to optimize the microgrid power flows for reduced operational costs and extended battery life. Morstyn et al. [8] developed a novel model predictive control (MPC) model to optimize the power flow among the distributed batteries such that the supply and demand are balanced and the operational costs are minimised. In addition, Sachs and Sawodny [9] designed a two-layer MPC method (the first layer optimizes energy dispatch between PV generation and power loads, while the second layer controls the power output from a diesel generator) for a hybrid microgrid system to minimize operational costs and enhance the system robustness against uncertainties from both supply and demand sides. All these approaches have demonstrated impressive performance in optimizing the power flows in a microgrid. However, as microgrid systems become more and more complex, such as the increase in the number of system variables and optimization objectives, these traditional approaches started incapable of expressing and effectively addressing the control optimization problems.

Recently, reinforcement learning (RL) has shown remarkable efficacy in optimizing the power management of complex microgrid systems attributed to its powerful model-free and self-learning capabilities [10]. For example, Ojand and Dagdougui [11] developed a two-stage MPC integrating a RL model (with a discrete state space) to control the distributed energy resources and power demand for the reduction of operational costs and enhancement of operating efficiency. However, a RL in this kind suffers from the curse of dimensionality, where the number of states grows exponentially with the increase of state variables. Deep reinforcement learning (DRL) overcomes this weakness by employing deep neural networks

Fulong Yao, Wanqing Zhao and Matthew Forshaw are with the School of Computing, Newcastle University, Newcastle Upon Tyne, NE4 5TG, UK. Yang Song is with the School of Mechanical and Electrical Engineering and Automation, Shanghai University, Shanghai, 200444, China. Corresponding author: Fulong Yao(F.Yao3@newcastle.ac.uk)

## Terminology

Abbreviations	Reinforcement Learning Symbols
RES	renewable energy sources
ESS	energy storage systems
PV	photovoltaic
RL	reinforcement learning
DRL	deep reinforcement learning
MDP	markov decision process
SGD	stochastic gradient descent
FC	fully connected
TD	temporal difference
WT	wind turbine
<b>Environment Symbols</b>	
$P_{g,t}$	imported power from national grid (kW)
$P_g^{max}$	pre-set maximum imported power from grid (kW)
$P_{b,t}$	power flowing into/out the battery (kW)
$P_{r,t}$	RES generation (kW)
$P_{d,t}$	aggregated power demand (kW)
$P_{u,t}$	unmet power (kW)
$PR_t$	market price (\$/kWh)
$CI_t$	carbon intensity (gCO <sub>2</sub> /kWh)
$E_{b,t}$	state of charge (kWh)
$E_b^{min}, E_b^{max}$	maximum and minimum state of charge (kWh)
$\Delta t$	time interval (h)
subscript $t$	time instant
$\eta_b$	charge/discharge efficiency of battery
$P_{b,sb}$	constant standby loss rate of the battery (kW)
<b>Parameters</b>	
$\epsilon$	random exploration rate
$K$	length of time series sequences in each episode
$\alpha$	coefficient of carbon benefits
$\beta$	coefficient of peak load limit
$\lambda$	coefficient of battery degradation
$w$	weight of Q Network
$w^-$	weight of Target Network
$M$	updating frequency for Target Network
$\tau$	updating rate of Target Network
$\gamma$	discount factor
$lr$	learning rate

to approximate the value functions for microgrid control, allowing it to handle larger and more complex microgrid environments with improved performance and efficiency [12]. For instance, Alabdullah and Abido [13] developed a deep Q network (DQN) approach, which considers the stochastic behaviors of supply & demand profile and pricing signals, to schedule the system operations and reduce costs. Yu et al. [14] further designed a double deep Q network (DDQN) for controlling energy storage systems, aiming to improving utilization of multiple renewable sources including PV, WT and hydrogen. These studies have demonstrated the vast potential and advantages of DRL for energy optimization in microgrids.

Furthermore, the robust learning capability of DRL has promoted the transition of microgrid control from a discrete state space to a more promising continuous state space. For example, Cao et al. [15] proposed a data-driven Noisy Net-Double Deep Q Network (NN-DDQN), which constructed a state space containing future market price and depth of charge as continuous variables, to optimize the battery energy arbitrage via load shifting. A data-driven online DRL method was devised in [16] to continuously control the microgrid using the past data (including power load, generations and electricity prices)

and current depths of battery. Harrold et al. [17] developed a DRL-based MPC algorithm that used the predicted future data (including market price, demand, PV and WT generations) to maximize the utilization of RES generations and reduce operational costs. These studies have shown that either historical or predicted further data can be incorporated to address complex control problems and yield favorable outcomes. However, there is an open question as to whether it is more beneficial to using future or past data when defining the microgrid state space for DRL.

The goal of balancing decarbonization, sustainability and cost-efficiency has now also posed another formidable challenge for power optimization in microgrid systems [18]. Optimizing the power management of microgrid systems only by relying on conventional considerations (such as market profit) is no longer sufficient to meet our decarbonization and sustainability commitments. Fortunately, recent research has begun to consider optimizing the power management from these two aspects. For example, Rangel et al. [19] designed an optimization model based on the formulation of a mixed-integer linear programming (MILP) to balance the fuel consumption, carbon emissions and operating costs of a Diesel-PV-Battery hybrid microgrid.

A cooperative operation model based on asymmetric nash bargaining was also developed in [20] for thermal-power hybrid microgrids to minimize the carbon emissions and power sharing operational costs. Moreover, Wang et al. [21] proposed a low-carbon optimal scheduling strategy for district microgrids. It employed a novel carbon emission measuring technique based on the flow analysis theory to calculate the power consumed by microgrids. However, existing research considering these multiple objectives in microgrid operations remains in its early stages. Optimizing the operational control of microgrid systems with a holistic view of environmental, infrastructural and economic considerations remains a challenge as it would bring more system complexities and dependencies (e.g. carbon intensity and its uncertainties).

To address the challenges posed by the uncertainties from both the supply and demand sides and by the complex interplay of decarbonization, sustainability and cost-efficiency, this paper proposes a holistic power optimization approach for microgrid control based on DRL. The ambition is to enhance the sustainability and reliability of the microgrid system, while simultaneously reducing operational costs and carbon emissions. To this end, the main contributions can be enumerated as follows:

1) A unified DRL framework is designed for microgrid control incorporating the influence of external and internal variables, as well as a new objective (reward) function to balance decarbonization, sustainability and cost-efficiency of the system.

2) A data-driven Double Dueling Deep Q Network (D3QN) architecture is devised to optimize the power management of microgrid systems integrated with RES and ESS.

3) Two data-driven control schemes (i.e. prediction-based and prediction-free) are formulated within the unified DRL framework to leverage the learning competencies of D3QN, offering better performance and flexibility in different operational circumstances.

The subsequent sections of this paper are structured as follows. Section II introduces the model of the microgrid with RES and ESS. Section III provides an overview of classic DRL algorithms. Section IV presents the proposed dynamic power optimization approach based on DRL, including the unified framework, a D3QN architecture and two data-driven control schemes. The experiments and performance evaluation are given in Section V, while conclusion is provided in Section VI.

## II. MICROGRID SYSTEM AND ITS MODELING

This paper considers the control-oriented power optimization for a large class of microgrid systems that integrate RES and ESS to meet the energy demand of a local community. The schematic of such a microgrid is depicted in Fig. 1, in which the arrows represent the direction of power/control/data flows. Here, energy can be supplied either from the national grid or RES (e.g. PV and WT), whilst the power load is the total electricity demand of the locality. Then, battery is employed as a

buffer to temporarily store renewable generations when there are surpluses after use, or to import electricity from the grid when the energy is cheap and clean. Therefore, an additional supply of energy (which is low-cost and low-carbon) can be created from battery for later use when there would be otherwise a need to import electricity from grid at a much higher price or carbon intensity.

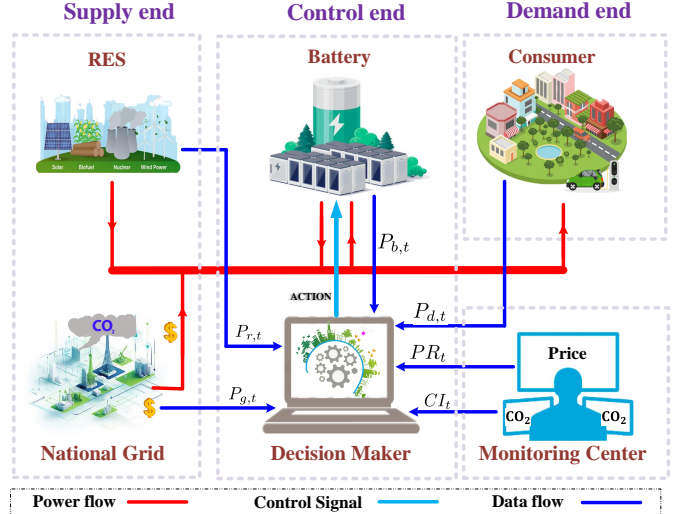


Fig. 1: The schematic of the microgrid

To model the above microgrid, the power balance problem between the supply and load can be first expressed as follows:

$$P_{g,t} + P_{b,t} + P_{r,t} - P_{d,t} = 0 \quad (1)$$

where  $t$  represents the time instant,  $P_{g,t}$  (kW) is the power imported from the national grid,  $P_{b,t}$  (kW) is the power flowing into/out the battery,  $P_{r,t}$  (kW) is the power generated by RES, and  $P_{d,t}$  (kW) is the aggregated consumer demand. The following constraints should be met:

$$P_{g,t} \geq 0 \quad (2)$$

$$P_{r,t} \geq 0 \quad (3)$$

$$P_{d,t} \geq 0 \quad (4)$$

$$\begin{cases} P_{b,t} > 0, & \text{if discharge;} \\ P_{b,t} = 0, & \text{if idle;} \\ P_{b,t} < 0, & \text{if charge.} \end{cases} \quad (5)$$

Then, we define the unmet power  $P_{u,t}$  (kW) as:

$$P_{u,t} = P_{d,t} - P_{r,t} \quad (6)$$

By substituting (6) into (1), this gives

$$P_{g,t} + P_{b,t} - P_{u,t} = 0 \quad (7)$$

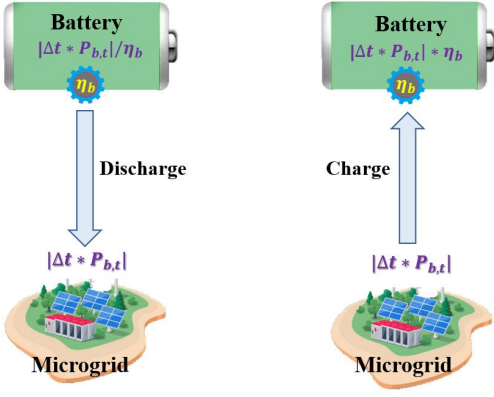


Fig. 2: Battery discharging and charging processes

Assuming the charge/discharge efficiency of battery is  $\eta_b \in (0, 1)$  and there are no other losses, the following holds:

$$\begin{cases} 0 < P_{b,t} * \Delta t \leq (E_{b,t} - E_b^{min}) * \eta_b, & \text{if discharge;} \\ P_{b,t} = 0, & \text{if idle;} \\ \frac{E_{b,t} - E_b^{max}}{\eta_b} \leq P_{b,t} * \Delta t < 0, & \text{if charge.} \end{cases} \quad (8)$$

where  $P_{b,t} * \Delta t * \eta_b$  (kWh) is the amount of charged energy within an interval  $\Delta t$  ( $P_{b,t} * \Delta t / \eta_b$  being the discharged energy),  $E_{b,t}$  (kWh) is the state of charge (SOC),  $E_b^{max}$  (kWh) and  $E_b^{min}$  (kWh) represent the maximum and minimum state of charge, respectively. Here, the processes of charging and discharging are illustrated in Fig. 2.

Therefore, the state transition of the battery is expressed as [22]:

$$E_{b,t+1} = \begin{cases} E_{b,t} - (\Delta t * P_{b,t}) / \eta_b, & \text{if } P_{b,t} > 0; \\ E_{b,t} - \Delta t * P_{b,sb}, & \text{if } P_{b,t} = 0; \\ E_{b,t} - \Delta t * P_{b,t} * \eta_b, & \text{if } P_{b,t} < 0. \end{cases} \quad (9)$$

$$P_{b,sb} \geq 0 \quad (10)$$

where  $P_{b,sb} \geq 0$  (kW) indicates a constant standby loss rate of the battery.

Additionally, to prevent potential damage to the grid, the long-term stable operation of the microgrid requires the imported power to meet the peak load constraint as much as possible:

$$P_{g,t} \leq P_g^{max} \quad (11)$$

where  $P_g^{max}$  (kW) represents the pre-set maximum peak load.

By substituting (7) into (11), the following is obtained:

$$P_{u,t} - P_{b,t} - P_g^{max} \leq 0 \quad (12)$$

The microgrid control system is required to make optimal decisions about when and how much to import power from the grid based on a number of variables, such as

RES generation, unmet power, SOC of battery, wholesale price and carbon intensity. Specifically, to achieve cost efficiency, decarbonization and sustainability, the microgrid is expected to:

- 1) buy as much power as possible and store it in the battery when the electricity price and carbon intensity are low;
- 2) give priority to use RES generations and the backup power in the battery to meet the demand when the price and carbon intensity are high;
- 3) limit the peak load and slow down battery degradation to ensure long-term security and sustainability of the microgrid.

### III. DEEP REINFORCEMENT LEARNING

#### A. Deep Q Network

Reinforcement learning (RL) is a machine learning paradigm where agents learn to make sequential decisions by interacting with an environment [23]. Despite its effectiveness in various applications, RL faces challenges in handling high-dimensional input spaces and addressing exploration-exploitation dilemma. Deep Q Network (DQN), developed by Google DeepMind [24], is a typical deep reinforcement learning (DRL) approach that combines deep neural networks with Q-learning (a typical RL algorithm) [25]. It addresses the limitations of traditional RL in discretizing environments involving high-dimensional state spaces. Generally, it uses a deep neural network to learn a control policy, which maps the states of the environment to optimal actions that maximize the expected cumulative reward over time [26]. In detail, the interaction between an agent and the environment can be modeled by a Markov Decision Process (MDP) with discrete time steps. This can be described by a tuple  $\{S, A, R, P_M, \gamma\}$  [27], where  $S$  represents the state space,  $A$  is the action space,  $R$  is the immediate reward,  $P_M(s_{t+1}|s_t, a_t)$  is the state transition probability which shows the probability that the agent would move to state  $s_{t+1}$  if it takes action  $a_t \in A$  in state  $s_t \in S$ , and  $\gamma$  is a discount factor that relates to the future reward and  $R$ .

Unlike the traditional Q-learning (which uses a table to store the expected values of the reward for each state-action pair), DQN adopts a deep neural network rather than a table to approximate the optimal value function  $Q^*(s_t, a_t)$ , as shown below:

$$Q(s_t, a_t; w_d) \approx Q^*(s_t, a_t) \quad (13)$$

where  $w_d$  is the network weights and  $s_t$  and  $a_t$  are the network inputs.

The optimal value function can be learnt through a number of successive interactions between the agent and environment. At each time step (interaction),  $Q(s_t, a_t)$  can be updated by a Bellman Equation [28], [29]:

$$Q(s_t, a_t) \leftarrow Q(s_t, a_t) + lr * [R_t + \gamma * \max_a Q(s_{t+1}, a) - Q(s_t, a_t)] \quad (14)$$

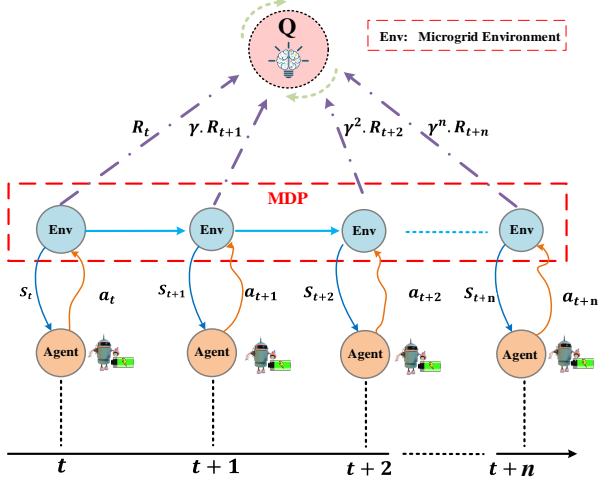


Fig. 3: The interaction process between the environment and the agent

where  $t$  denotes the time step,  $lr$  is the learning rate,  $\gamma$  is the discount factor used to balance the importance between the immediate reward ( $R_t$ ) and the potential future reward ( $\max_a Q(s_{t+1}, a)$ ) of an action. A higher value of  $\gamma$  means that future rewards are more certain and valuable. Here,  $R_t + \gamma * \max_a Q(s_{t+1}, a)$  is also called the TD target. The whole interaction process between a microgrid environment and the agent can be illustrated in Fig. 3.

The flowchart of the learning process of DQN is shown in Fig. 4. The objective is to minimize the Mean Squared Error  $L(w_d)$  between the network output  $Q(s_t, a_t; w_d)$  and TD target  $R_t + \gamma * \max_a Q(s_{t+1}, a; w_d^-)$ :

$$L(w_d) = (R_t + \gamma * \max_a Q(s_{t+1}, a; w_d^-) - Q(s_t, a_t; w_d))^2 \quad (15)$$

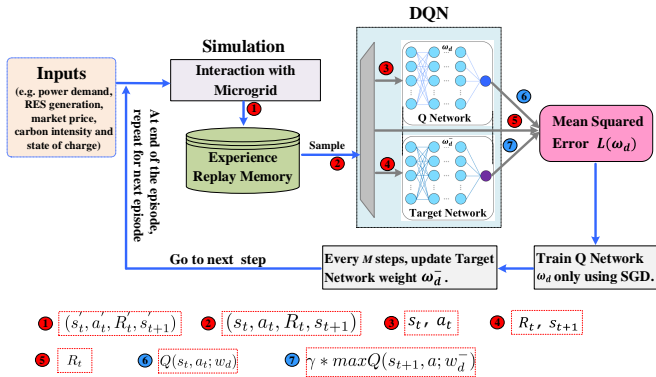


Fig. 4: Flowchart of the learning process of DQN (adapted from [24])

Here, a separate Target Network with weights  $w_d^-$  is used to estimate the TD target value [30]. Generally, the Target Network weight  $w_d^-$  is temporarily fixed while Q

Network is under training with stochastic gradient descent (SGD) [31], but it will be then periodically updated based on the Q Network weight  $w_d$  (i.e. directly copy  $w_d$  to  $w_d^-$  every  $M$  steps). Moreover, an experience replay component is employed to store the interaction experiences ( $s'_t, a'_t, R'_t, s'_{t+1}$ ) with the microgrid environment in a replay memory so that the agent then randomly samples mini-batches from the memory to update the network weights. In this way, the replay allows the agent to reuse past experiences and breaks the sequential correlations, enhancing the diversity and efficiency of learning [32].

## B. Variants of DQN

1) *Double Deep Q Network (DDQN)*: DDQN extends the DQN algorithm and aims to address the issue of overestimation of Q-values [33]. In traditional DQN, a network is used for both estimating the expected values and selecting actions. This can easily lead to overestimation of Q-values, especially in situations where there are multiple highly ranked actions. DDQN has proven to be an effective way to alleviate the overestimation issue by introducing a new DQN network to separate the value estimation from action selection. Generally, DDQN adopts one DQN with weight  $w_{dd}$  to select the best action at current state and then uses the other DQN with weight  $w_{dd}^-$  to estimate the target Q value based on the selected action. The objective of DDQN can be expressed as [33],

$$L(w_{dd}) = (R_t + \gamma * Q(s_{t+1}, \underset{a}{\operatorname{argmax}} Q(s_{t+1}, a; w_{dd}); w_{dd}^-) - Q(s_t, a_t; w_{dd}))^2 \quad (16)$$

2) *Dueling DQN*: Dueling DQN, introduced by Wang et al [34], is another variant of DQN that focuses on improving the learning and representation of action-value functions. In traditional DQN, the Q-values are directly estimated for each action in a given state. However, in many cases, different actions may have similar values and it is unnecessary to estimate their values individually [35]. Dueling DQN addresses this issue by decomposing the Q-value into two components: a state-value function  $\mathcal{V}(s)$  that represents the expected value of being in a particular state (regardless of the action taken) and an advantage function  $\mathcal{A}(s, a)$  that shows the relative significance of each action over other actions. The state-value function is responsible for estimating the baseline value for each state, while the advantage function quantifies the additional value offered by taking a particular action.

Rather than relying on one stream of fully connected (FC) layers to estimate the Q-values, the dueling DQN employs two streams of FC layers to calculate the value function  $\mathcal{V}(s)$  and advantage function  $\mathcal{A}(s, a)$ , respectively. These two streams are then combined to produce a Q-value for each action, which can be represented as [34]:

$$Q(s, a) = \mathcal{V}(s) + \mathcal{A}(s, a) - \frac{1}{|A|} \sum_{a' \in A} \mathcal{A}(s, a') \quad (17)$$



#### IV. D3QN-BASED OPTIMIZATION APPROACH

Considering the large number of states in the continuous space for microgrid modeling, this paper proposes a holistic data-driven power optimization approach based on DRL for controlling the battery charging and discharging behaviors. Fig. 5 shows the framework of the proposed approach, in which two data-driven control schemes are designed to formulate the control problem within a MDP. Then, a D3QN architecture is developed to optimize the power flow for real-time energy management.

##### A. MDP Definition

In this paper, the main goal for the agent is to control the behavior of battery to reduce operational costs and carbon emissions as well as improving sustainability. First, the following microgrid MDP with discrete actions and continuous states is defined.

1) *Action space*: The action space is discretized as (18) in which the behaviors  $a_t \in A$  can be maximum charge (-1), half charge (-0.5), idle (0), half discharge (0.5) and maximum discharge (1), respectively.

$$A = \{-1, -0.5, 0, 0.5, 1\} \quad (18)$$

These actions are relative values to the maximum amount of electricity ( $E_{max}$  (kWh)) that can be transported to/from battery within an interval  $\Delta t$ . Thus, the resultant charged/discharged power can be computed by (19). It should be noted that  $P_{b,t}$  is also required to meet the constraint in (8).

$$P_{b,t} = \frac{a_t * E_{max}}{\Delta t} \quad (19)$$

$$E_{max} \geq 0 \quad (20)$$

2) *State space*: The continuous state space consists of two parts: the external variables (including market price, carbon intensity and unmet power) that are not controlled by the agent; and the internal variable (SOC of battery) that can be controlled via the aforementioned actions. In this paper, two data-driven control schemes (i.e. prediction-based and prediction-free) are employed to formulate the control problem, which are illustrated as follows:

① *Prediction-based (PB) scheme*: We employ the MPC concept where the predicted near future statuses of the external variables are used in combination with battery status ( $E_{b,t}$ ) to form the state space, as expressed in (21). The idea is to find the optimal control strategy for the current time step but taking into account future changes to the system. It should be noted that this paper only focuses on the controller design, while the prediction itself is beyond the scope of this paper.

$$s_t = (PR_t, PR_{t+1}, \dots, PR_{t+T}, CI_t, CI_{t+1}, \dots, CI_{t+T}, P_{u,t}, P_{u,t+1}, \dots, P_{u,t+T}, E_{b,t}) \quad (21)$$

Here,  $T$  indicates the time horizon to be considered for each variable,  $PR_t$  is the wholesale price (\$/kWh), and  $CI_t$  (gCO2/kWh) is the carbon intensity.

② *Prediction-free (PF) scheme*: As the name suggests, this scheme doesn't require a prediction model. Instead, it replaces predicted values with historical records for the external inputs in the state space. The idea is to implicitly capture the trend of variations in the external variables and incorporate them into the inference of control actions. In this case, the state space is defined as (22). This scheme can effectively reduce the complexity of the control solution and avoid prediction uncertainties.

$$s_t = (PR_{t-T}, \dots, PR_{t-1}, PR_t, CI_{t-T}, \dots, CI_{t-1}, CI_t, P_{u,t-T}, \dots, P_{u,t-1}, P_{u,t}, E_{b,t}) \quad (22)$$

It can be seen from (21) and (22) that merging the demand  $P_{d,t}$  and RES generation  $P_{r,t}$  together as the unmet power  $P_{u,t}$  greatly reduces the input dimension, from a space of  $4(T+1) + 1$  to  $3(T+1) + 1$ .

3) *Reward function*: Given the main goal of this work, the reward function should reflect not only operational costs and carbon emissions, but also the reliability and sustainability of the microgrid. The immediate reward  $R_t$  given an action at time step  $t$  is defined as follows to account for market profit, carbon benefit, peak load and battery degradation, respectively.

$$R_t = PR_t * P_{b,t} * \Delta t + \alpha * CI_t * P_{b,t} * \Delta t + \beta * \min[0, P_{b,t} + P_g^{max} - P_{u,t}] * \Delta t - \lambda * |a_t| * E_{max} \quad (23)$$

where  $\alpha \geq 0, \beta \geq 0, \lambda \geq 0$  are the weights controlling the importance of each objective. It should be noted that  $PR_t$  and  $CI_t$  should be scaled to  $[0,1]$  during learning, while other variables remain unchanged.

Here, we can view from the first two items that market profits and carbon benefits are essentially the reductions in operational costs and carbon emissions due to adopting appropriate actions. Generally, the more the battery discharges at high price and carbon intensity ( $P_{b,t} > 0$ ), the less the system generates operational costs and carbon footprints. The third item indicates the penalty for breaking the peak load constraint. The use of mathematical operators ( $\min$ ) guarantees that it will only apply when the instantaneous imported power is greater than the maximum allowed. The last item is related to the battery degradation cost which is simplified as a linear function proportional to charging and discharging actions.

In addition, the weights in the reward function need to be carefully chosen based on practical considerations. In this paper, we considered the objectives in the following order: (i) increased market profits and the safe and sustainable operation of the microgrid, (ii) carbon emission reduction and (iii) extended battery life. In particular, as battery degradation is a cumulative process and a single charge/discharge event has only a small effect on it. Therefore,  $\lambda$  should be chosen as a small value in

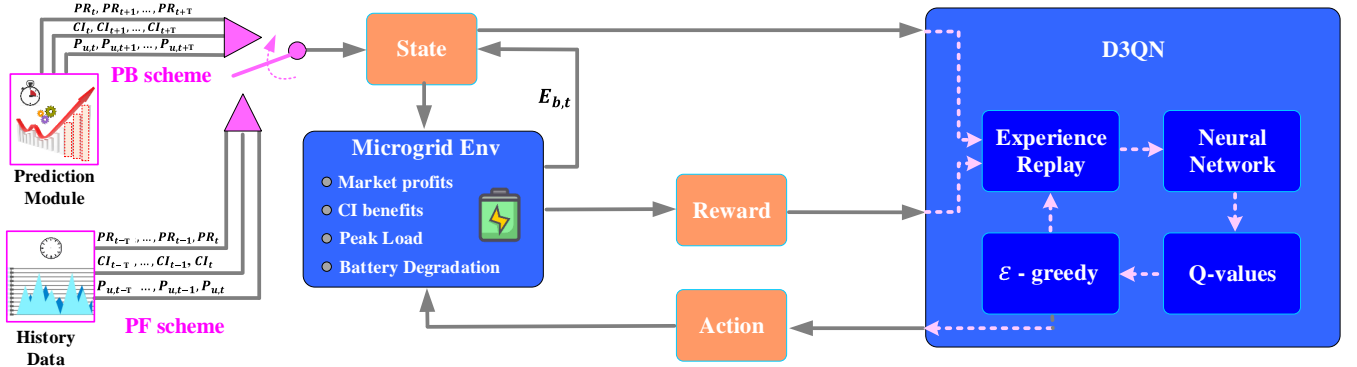


Fig. 5: The framework of the proposed D3QN-based approach

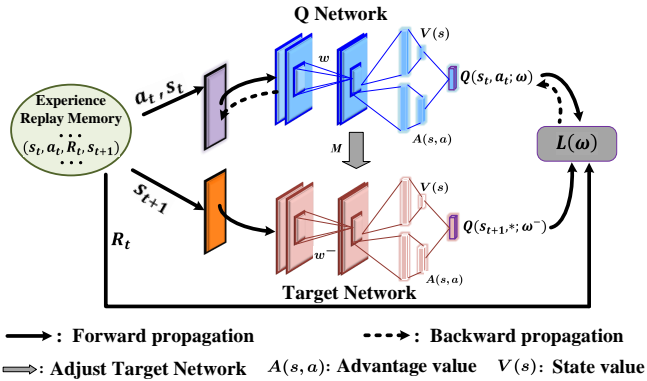


Fig. 6: The architecture of D3QN

the reward calculation to reflect this subtle effect. Given these considerations, the coefficients in the reward function should meet the following constraint.

$$\beta > 1 > \alpha \gg \lambda \geq 0 \quad (24)$$

### B. D3QN-based Approach

A data-driven Double Dueling DQN (D3QN) architecture is developed in this paper, which combines the advantages of DDQN and Dueling DQN together to optimize microgrid controls. The architecture of this D3QN is shown in Fig. 6. In the forward propagation, a mini-batch of experience tuple  $(s_t, a_t, R_t, s_{t+1})$  is sampled from the experience replay memory. Then, the present state  $s_t$  and action  $a_t$  are passed to the Q Network to estimate the expected total reward  $Q(s_t, a_t; w)$ , while the next state  $s_{t+1}$  is passed to approximate a Target Network to calculate the future reward  $Q(s_{t+1}, *; w^-)$ . Noted that the target network is simply a copy of the Q network but updated every  $M$  time steps to ensure the stability of the learning process. Based on the TD algorithm [28], to update the Q network, the loss  $L(w)$  can be computed based on the difference between  $Q(s_t, a_t; w)$  and  $\gamma * Q(s_{t+1}, *; w^-) + R_t$  (the latter is the sum of future and immediate rewards

from the underlying action). In the backward propagation,  $L(w)$  is then minimised by updating the weights  $w$  in the Q Network. Moreover, the weights  $w^-$  of the Target Network will only get updated every  $M$  time steps using the weights  $w$  from the Q network. Differing from the traditional DQN where the  $w^-$  is adjusted by hard update (directly copying  $w$  as  $w^-$ ), this paper used the soft update (25) to adjust the target weights  $w^-$ .

$$w^- = (1 - \tau) * w^- + \tau * w \quad (25)$$

Here,  $\tau$  is the updating rate of the weights  $w^-$ . The employment of soft updates not only helps strike a balance between exploration and exploitation of the learning, but also enhances stability and facilitates experience accumulation.

The flowchart of the D3QN-based optimization approach for microgrid control can be illustrated in Fig. 7, while the implementation steps are depicted in Algorithm 1. Overall, the learning process is carried out over a number of episodes. In each episode, a total of  $K$  time series sequences are first sampled from the whole dataset and used as inputs to the proposed approach. Here, each time series is made up of a sequence of  $3(T + 1)$  external inputs plus an internal variable to represent the state in (21) and (22). By simulating the microgrid system one step forward, each time series will produce a tuple  $(s'_t, a'_t, R'_t, s'_{t+1})$ , where  $a'_t$  can be obtained using the  $\epsilon$ -greedy algorithm with the optimal policy  $\pi^*$ . The system can thereby receive an immediate reward  $R'_t$  (23) and move to the next state of charge  $E'_{b,t+1}$  (9). This tuple will be stored in the experience replay memory for later use. Subsequently, a mini-batch of tuple  $(s_t, a_t, R_t, s_{t+1})$  will be randomly sampled from the experience replay memory to update the optimal policy  $\pi^*$  using the D3QN network as described above. The updated  $\pi^*$  will be then used in microgrid simulation to decide the action of the next time series. The learning continues until a maximum number of episodes is reached, where the optimal Q network is obtained. In applying the control actions, this paper implemented the  $\epsilon$ -greedy strategy with a decreasing  $\epsilon$

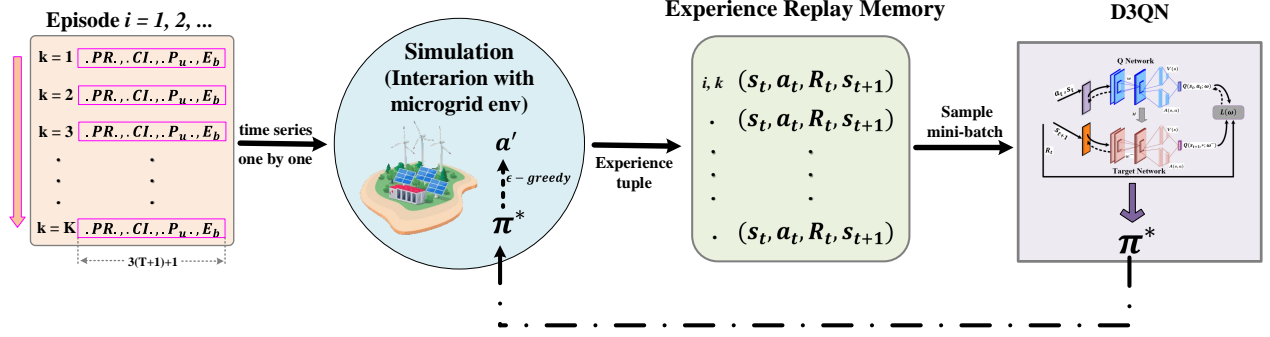


Fig. 7: Flowchart of the D3QN-based approach

using an exponential decay factor of 0.999. The minimum value of  $\epsilon$  was truncated to 0.01 ( $\epsilon$  was also fixed as 0.01 for the application of the optimized Q network). This enables the agent to freely explore the microgrid environment at the beginning and then gradually rely on the learned knowledge and experience while still having the chance to further improve the obtained policy in question.

## V. SIMULATIONS AND PERFORMANCE EVALUATION

### A. Microgrid Description and Parameter Configuration

The proposed approach was evaluated using an open-source dataset for an integrated district energy system in US [37], which contains hourly load, market price and PV generation for one year. In addition, the hourly carbon intensity data was collected from the WattTime API [38]. The WattTime API offers access to carbon intensities of electrical grids in different regions of the world. Some pre-processing tasks (such as scaling and cleaning) were also performed on the integrated dataset, which was made accessible on Github [39].

As defined by the granularity of the dataset, the time interval is  $\Delta t = 1h$  and the time horizon of the PB and PF schemes was set as  $T = 24$ . In other words, this paper treats the microgrid control problem as using the data of the future/past 24 time steps to determine the charging or discharging actions. Generally, the battery capacity  $E_b^c$  in a microgrid is designed to be much smaller than the peak unmet energy due to the high capital and maintenance costs, while the charging/discharging rate should ensure that the battery can theoretically be fully charged or discharged within a limited time [15], [40]. Table I lists the configurations of the microgrid considered in this paper. According to [41], lithium-ion batteries may fail when overcharged or over-discharged, and can even explode in extreme cases. To maintain the security of the microgrid, the maximum ( $E_b^{max}$ ) and minimum ( $E_b^{min}$ ) states of charge are thus defined as:

$$\begin{cases} E_b^{max} = 0.9 * E_b^c \\ E_b^{min} = 0.1 * E_b^c \end{cases} \quad (26)$$

---

### Algorithm 1: D3QN-based Approach for Microgrid Control

---

**Input** : predicted future or historical data -  $PR, CI, P_u, E_b$

**Output** : optimal policy  $\pi^*$  (Q network)

**Procedure:**

- 1 Initialize microgrid configurations and experience replay memory;
  - 2 Initialize parameters and network weights ( $w^-, w$ );
  - 3 **for**  $i = 1$  to  $Episode_{max}$  **do**
  - 4     Randomly initialize  $E_{b,t}$  within  $[E_b^{min}, E_b^{max}]$ ;
  - 5     Sample a sequence containing K time series from the whole dataset;
  - 6     **for**  $k = 1$  to  $K$  **do**
  - 7         Observe the state  $s'_t$  based on (21) or (22) ;
  - 8         Select and execute an action  $a'_t$  using Q Network based on  $\epsilon$ -greedy;
  - 9         Calculate reward  $R'_t$  using (23) and  $E_{b,t+1}$  using (9);
  - 10         Observe the next state  $s'_{t+1}$ ;
  - 11         Store the tuple  $(s'_t, a'_t, R'_t, s'_{t+1})$  in the Experience Replay Memory;
  - 12         Randomly sample a mini-batch of  $(s_t, a_t, R_t, s_{t+1})$  from Replay Memory;
  - 13         Estimate the  $Q(s_t, a_t; w)$  using Q Network with  $s_t$  and  $a_t$ ;
  - 14         Calculate the TD target using Target Network with  $s_{t+1}$  and  $R_t$ ;
  - 15         Calculate loss  $L(w)$  using (16) and (17);
  - 16         Optimize the weights  $w$ ;
  - 17         **if**  $k \bmod M = 0$  **then**
  - 18             Soft update the weights  $w^-$  of Target Network using (25);
-



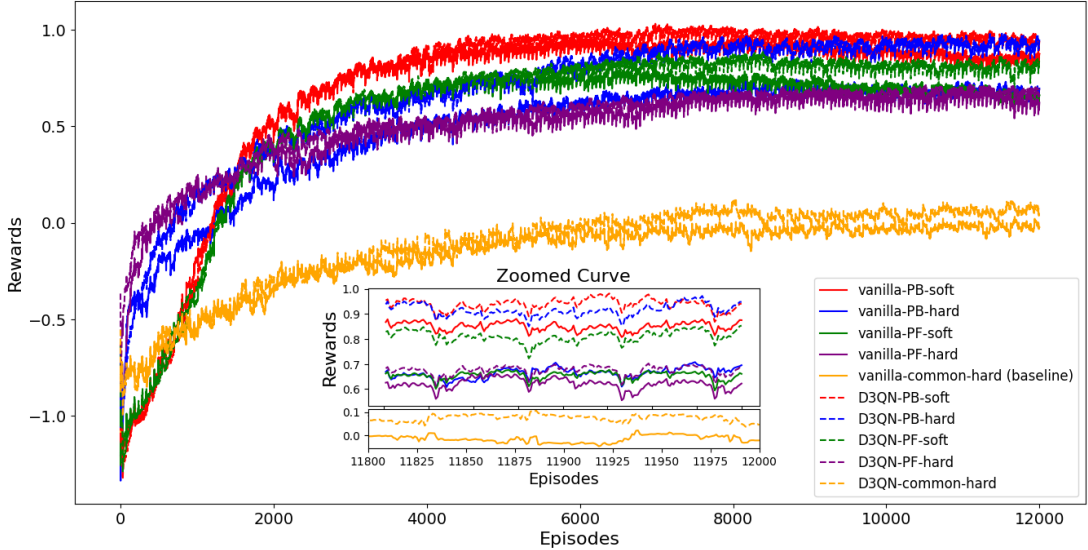


Fig. 8: The evolution of rewards during the training stage

TABLE I: Configuration of the microgrid

Item	Value	Unit	Item	Value	Unit
$E_b^c$	1000	kWh	$E_{max}$	300	kWh
$E_b^{max}$	900	kWh	$\eta_b$	0.95	—
$E_b^{min}$	100	kWh	$P_g^{max}$	4450	kW
$\Delta t$	1	h	$T$	24	—

In the proposed D3QN, the same Q-network structure (exclude input and output layers) was adopted for both the value function and advantage function streams. The structure and parameter settings of the Q network designed in this paper are shown in Table II. The update frequency for the Target Network was set as  $M = 24$  to be aligned with the number of hours in one day, while the length of time series sequences in each episode was set as  $K = 168$  to be equal to the number of hours in a week. In other words, we train the D3QN on a week's worth of samples in each episode, updating the Q Network for each sample (hour) and updating the Target Network every day (24 hours). Moreover, after some trial and error, the parameters in the reward function (23) were set as:  $\alpha = 0.25, \beta = 1.5, \lambda = 0.02$ .

To fully evaluate the effectiveness of the proposed D3QN approach, this paper provides a comprehensive comparison between vanilla (traditional) DQN and D3QN, PB and PF schemes, and hard and soft updates. Also, the vanilla DQN (hard update) together with the common data-driven scheme (where only the current data ( $PR_t; CI_t; P_{u,t}$ ) is used to infer actions from a policy) was adopted as the baseline to examine the superiority of the proposed approach. The implementation was coded in Python using the Keras library and was run on Google Colab with high RAM and no hardware accelerators.

TABLE II: Structure and parameter settings of the network (each stream)

Item	Value
no. of FC layers	3
no. of neurons per FC layer	64
update frequency of Target Network: $M$	24
length of time series sequences: $K$	168
updating rate of Target Network: $\tau$	0.01
batch size	64
learning rate	0.0003
discount factor: $\gamma$	0.99
random exploration: $\epsilon$	$0.3 \rightarrow 0.01$
activation function	Relu
optimizer	Adam

### B. Convergence Evaluation

The convergence of the proposed microgrid control approach is first evaluated in this subsection. The convergence curves of vanilla DQN and D3QN under different implementations are shown in Fig. 8. To visualise the learning process more clearly, the cumulative reward for each episode (scaled down by 1000 times) is the average of the past 50 episodes. Due to the fact that each episode is only equivalent to a period of consuming 168-hour data (one week) and the random exploration  $\epsilon$  is eventually truncated at 0.01, it is reasonable to see the converged reward fluctuates within a certain range. Table III presents the average and variance of the converged reward of the 10 approaches during 10,000-12,000 episodes. Under the same or similar learning conditions, the following can be observed:

- 1) PB and PF schemes (whether in the vanilla or D3QN architectures) both substantially outperformed the common data-driven scheme, indicating the validity of bringing either historical or predicted data of the exter-

TABLE III: Converged rewards (average and variance) from different microgrid control approaches

Approach	Variance (Reward)	Average (Reward)
Vanilla-PB-soft	0.00027	0.8509
Vanilla-PB-hard	0.00043	0.6639
Vanilla-PF-soft	0.00024	0.6549
Vanilla-PF-hard	0.00048	0.6215
<b>D3QN-PB-soft</b>	<b>0.00047</b>	<b>0.9392</b>
D3QN-PB-hard	0.00055	0.9158
D3QN-PF-soft	0.00050	0.8109
D3QN-PF-hard	0.00029	0.6752
D3QN-common-hard	0.00020	0.0753
<b>Vanilla-common-hard*</b>	<b>0.00023</b>	<b>-0.0155</b>

\* means the baseline

nal variables into the state space. The control actions can thereby be more proactive to future changes of the microgrid system rather than only reactive to its current statuses.

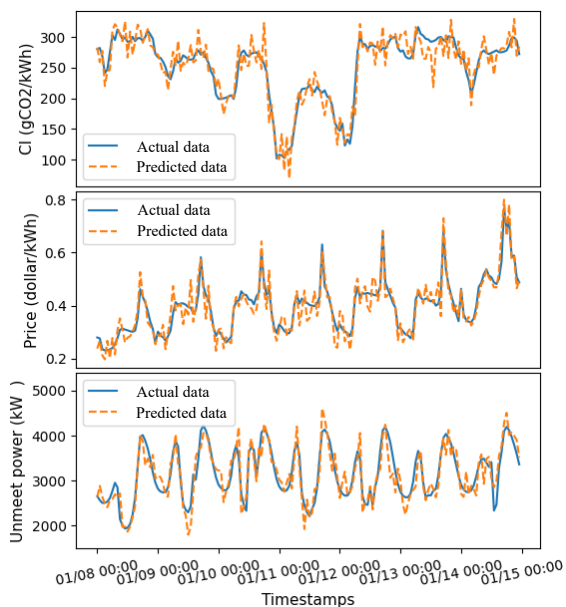


Fig. 9: An illustration of the actual values and simulated predictions with 10% noise.

2) The PB scheme (when assuming the prediction was 100% accurate) was more likely to achieve higher rewards than the PF scheme, either on vanilla or D3QN architecture.

3) Although the structure of D3QN is more complex than vanilla's, it offered much greater rewards.

4) Compared with hard update, although soft update progressed slower in the initial learning stage, it eventually reached convergence almost at the same time as the former and obtained a higher reward.

5) The stability of 10 approaches was demonstrated by the relatively small variance compared to the average of rewards.

### C. Cumulative Reward Evaluation

To further validate the effectiveness of the proposed approach, the cumulative reward over the whole learning period (i.e. one year given this dataset) is also evaluated on both actual values and simulated predictions. Here, the predictions of external variables were generated by adding Gaussian noises to the actual values, with a mean of 0 and a variance equal to 10% of the actual data, an illustrative example being given in Fig. 9. This was to introduce randomness and uncertainty to make the predicted future values more realistic. The simulation results against the actual and predicted values are respectively shown in Fig. 10 and Fig. 11. It is worth noting that the PF scheme does not rely on predictions, its results being kept in Fig. 11 for the convenience of comparisons. Additionally, Table IV gives the cumulative rewards received in both actual and predicted cases.

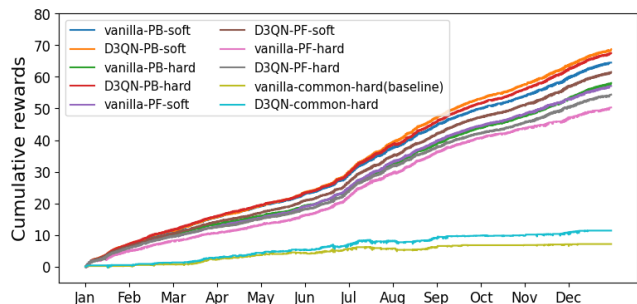


Fig. 10: Experimental results using the actual values of external variables

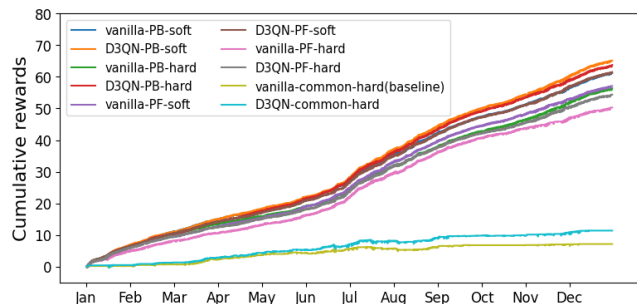


Fig. 11: Experimental results using the simulated predictions of external variables

The observations from the two figures reveal the following:

1) The D3QN-PB-soft approach achieved the best results in using both actual and predicted values, which is

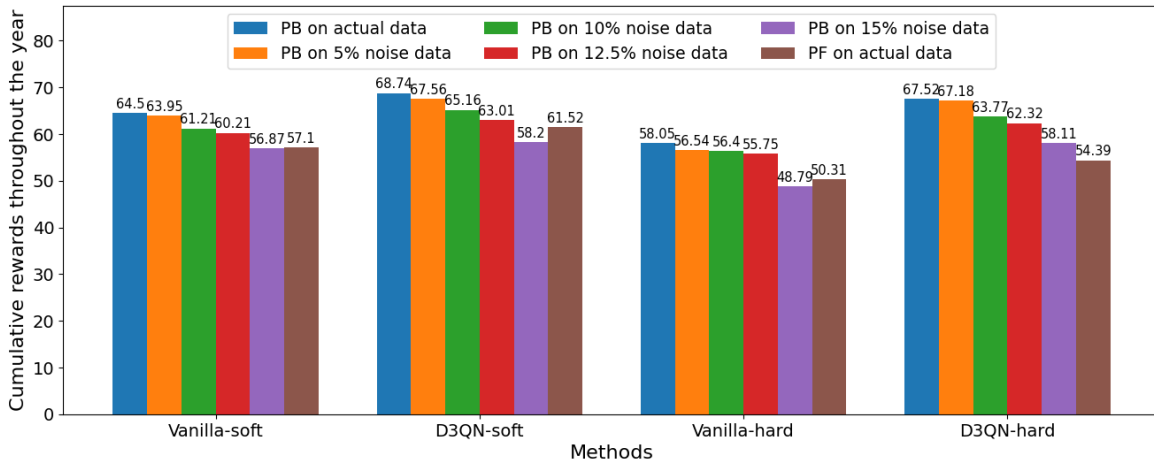


Fig. 12: Comparative results between using the actual and noisy data at different levels

TABLE IV: Cumulative rewards in actual and predicted datasets (\* means the baseline)

Approach	Actual	Predicted
Vanilla-PB-soft	64.50	61.21
Vanilla-PB-hard	58.05	56.40
Vanilla-PF-soft	57.10	—
Vanilla-PF-hard	50.31	—
<b>D3QN-PB-soft</b>	<b>68.74</b>	<b>65.16</b>
D3QN-PB-hard	67.52	63.77
D3QN-PF-soft	61.52	—
D3QN-PF-hard	54.39	—
D3QN-common-hard	11.37	0.0753
<b>Vanilla-common-hard*</b>	<b>7.13</b>	<b>-0.0155</b>

consistent with the conclusions drawn in Section V-B (i.e. PB, D3QN and soft update were all more in favour of producing higher cumulative rewards).

2) Both PB and D3QN tended to have more improvement upon the policy learning than soft update. In detail, the D3QN-PB-soft approach produced a cumulative reward that is 1.8% (using the actual as predictions) and 2.2 % (using noise data as predictions) higher than that of D3QN-PB-hard, showing a slight improvement of soft update. In contrast, the D3QN-PB-soft approach got 11.7% (actual) and 5.9% (noise) higher cumulative rewards than that of D3QN-PF-soft, and 6.6% (actual) and 6.5% (noise) higher cumulative rewards than that of vanilla-PB-soft, which demonstrated remarkable improvements of PB and D3QN.

3) With 10% noise introduced to the prediction, the performance of the PB scheme declined significantly, though D3QN-PB (either with soft or hard update) still performed the best compared to other approaches.

#### D. Comparison between control schemes and with other DRL methods

As the performance of PB scheme is proportional to the prediction accuracy of external variables, this paper further evaluates PB’s resilience to prediction uncertainty (i.e. prediction errors). In addition to the 10% Gaussian noise added before, we also studied the situations where predictions came with 5%, 12.5% and 15% errors, respectively, as shown in Fig. 12. For the convenience of comparison, the results of the PF scheme are kept here again. The results indicate that the PB scheme outperforms the PF scheme when the prediction error is within 12.5%. However, for errors exceeding 12.5%, the PF scheme becomes more advantageous not only because it has a higher return, but also because it avoids the need to design additional predictive models.

In previous subsections, we have comprehensively discussed the superiority of our approach compared to traditional DQN (vanilla DQN). Here, we further compared the D3QN-based optimization approach with other popular DRL-based optimization methods, including DDQN, Duling DQN, NN-DDQN. The three methods have been widely used to solve similar microgrid control problems and achieved remarkable results, as described in [14], [15], [42]. Fig. 13 and Fig. 14 show the comparison of annual cumulative rewards using actual and predicted values, respectively. The quantified annual cumulative rewards are listed in Table V. Here, it can be observed that our approach is much better than the other three methods whether using the actual values or the predicted values (10% noise). This holds true for both the PB and PF schemes.

#### E. Objectives Evaluation

This subsection is to assess each individual objective within the reward function, i.e. market profits, carbon benefits, battery degradation and peak load constraint. We took D3QN-PB-soft approach to demonstrate this

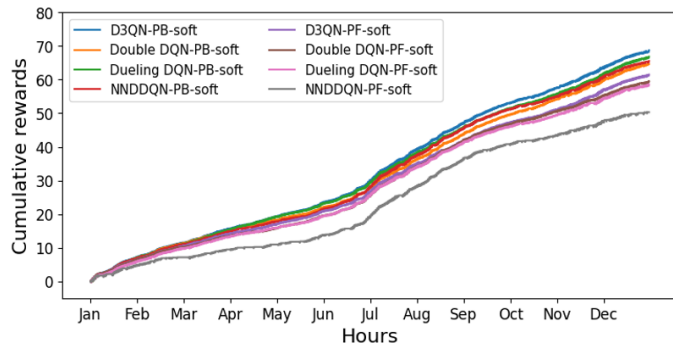


Fig. 13: Comparison with other DRL methods using actual values

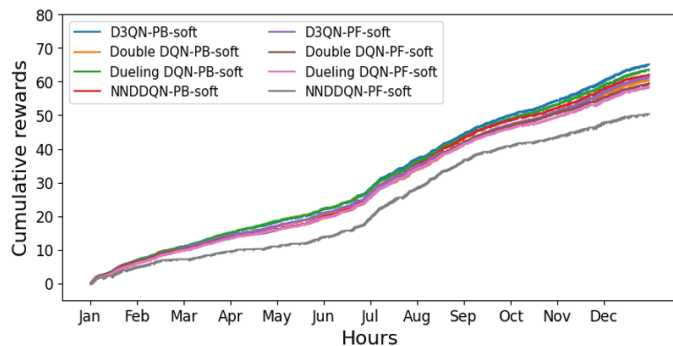


Fig. 14: Comparison with other DRL methods using predicted values

TABLE V: Annual cumulative rewards of different methods

Approach	Actual	Predicted
<b>D3QN-PB-soft</b>	<b>68.74</b>	<b>65.16</b>
Double DQN-PB-soft	64.67	60.55
Dueling DQN-PB-soft	66.85	63.62
NN DDQN-PB-soft	65.56	62.13
<b>D3QN-PF-soft</b>	<b>61.52</b>	—
Double DQN-PF-soft	59.54	—
Dueling DQN-PF-soft	58.63	—
NN DDQN-PF-soft	50.31	—

objective evaluation as it produced the best rewards in various scenarios presented previously. Fig. 15 - Fig. 18 show the cumulative values of each objective over the year on actual and predicted data (10% noise). The proposed approaches without considering each of the objectives are also presented there for comparison.

As discussed in Section IV-A-3), the market profits and carbon benefits are essentially the reductions in operational costs and carbon emissions due to adopting appropriate actions. It, therefore, can be seen that the inclusion of each objective in the reward function all played a positive role in controlling the decarbonization, sustainability and cost-efficiency of the microgrid.

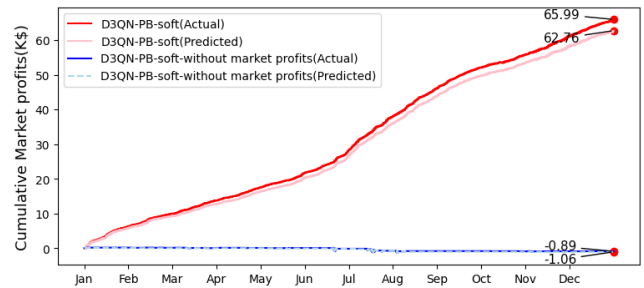


Fig. 15: The actual values of market profits over the year on actual and predicted data

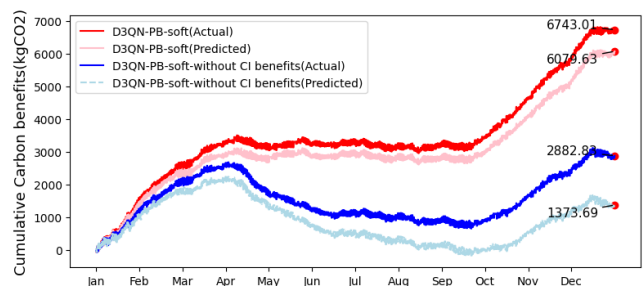


Fig. 16: The actual values of carbon benefits over the year on actual and predicted data

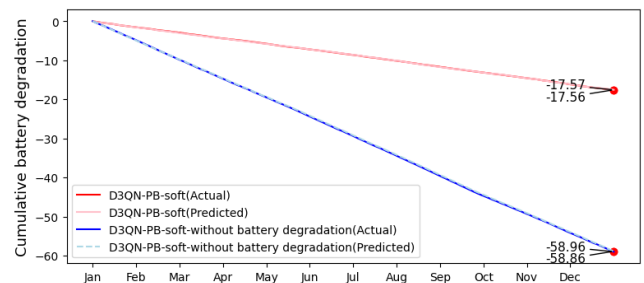


Fig. 17: The actual values of battery degradation over the year on actual and predicted data

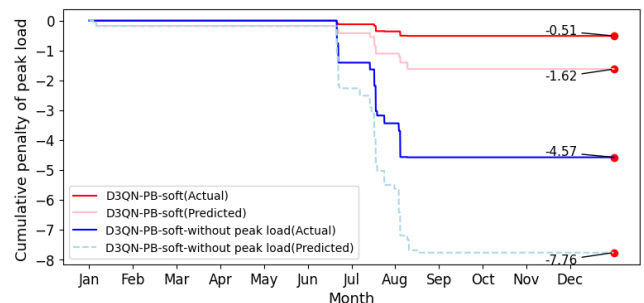


Fig. 18: The actual values of peak load over the year on actual and predicted data

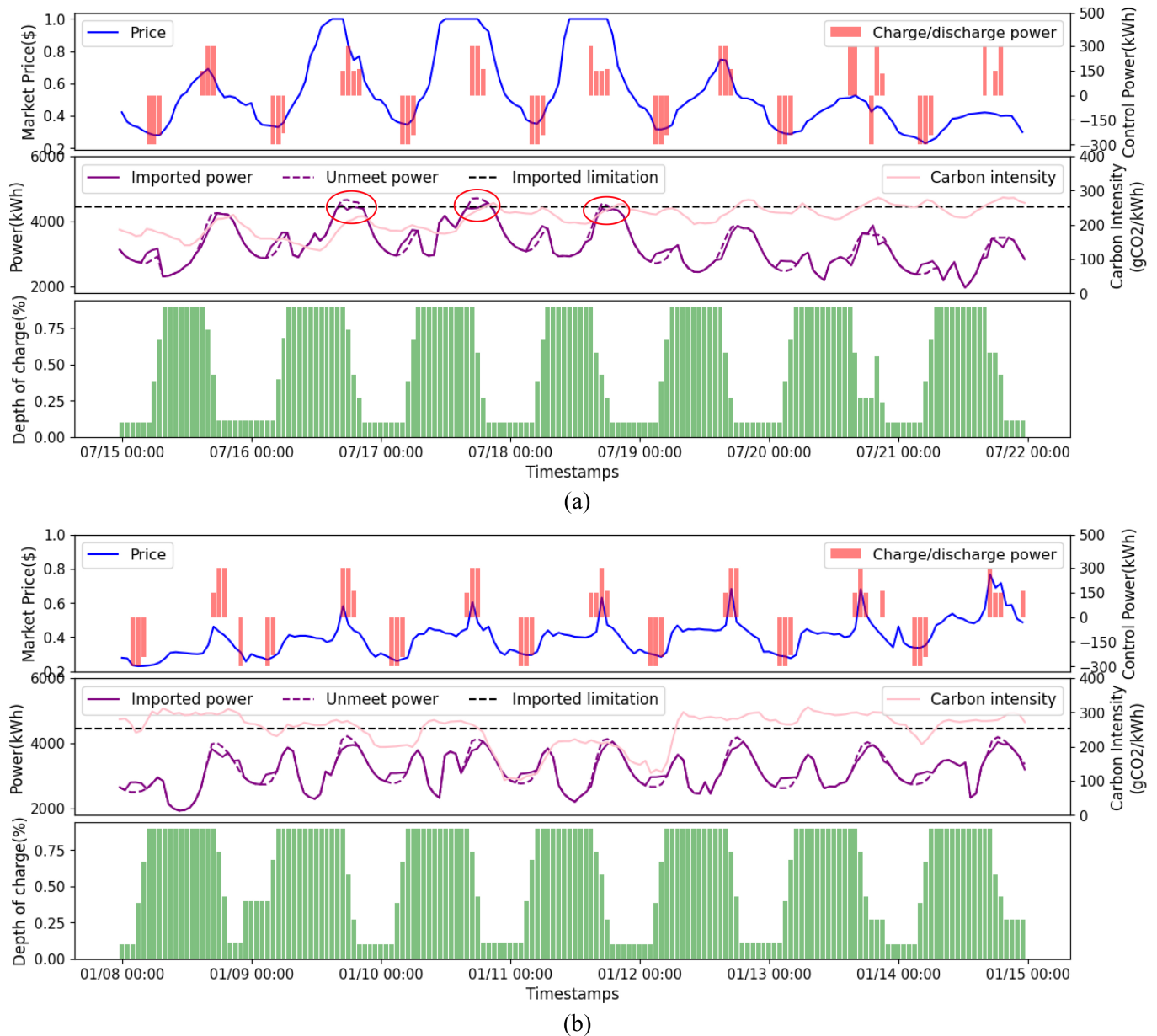


Fig. 19: A week-long visualization of battery behaviors in summer (a) and winter (b)

Specifically, the proposed D3QN-PB-soft approach can effectively control battery behaviors to reduce carbon emissions and operational costs. Specifically, this approach with a holistic reward function reduced the operational costs by 7514.61% and carbon emissions by 133.90% on the actual dataset (6020.75% and 342.58% respectively, on the predicted data) - see Fig. 15 and 16. As also shown in Fig. 17 and 18, the proposed approach successfully reduced the battery degradation and peak load.

In addition, some interesting observations can be drawn between different objectives and seasons. For example, the carbon benefit exhibited higher sensitivity during the winter, whereas the market profit showed greater sensitivity during the summer. The peak load exceeded the limit only during specific periods in the summer, while

battery degradation was relatively insensitive to seasonal variations.

#### F. Simulation Visualization

To further demonstrate the effectiveness of the proposed approach (again taking D3QN-PB-soft as an example), Fig. 19 shows the resultant charging and discharging behaviour of the battery (one week in summer and winter, respectively). It can be seen that the control strategy was not only suitable for the winter - see Fig. 19 (b), but can also be effective in the summer when the variation of market price and unmet power were quite high - see Fig. 19 (a). This means that the proposed approach can effectively guide the agent to charge during low price and carbon intensity periods as well as to discharge during



high price and carbon intensity periods in both seasons. When the unmet power exceeded the maximum import constraint in summer, the agent can promptly control the battery to adopt a discharge strategy to ease the peak load pressure - see the peak hours between 07/16 and 07/18 (marked by red circles). In addition, as the charging and discharging operations need to meet the battery's constraints (8), some charging behaviors other than the five specified ones reasonably appeared in the simulation.

## VI. CONCLUSION

This paper presented a holistic data-driven power optimization approach based on D3QN to manage the operational control of the integrated energy systems. The proposed approach was able to handle multiple economic, environmental and network considerations, plus proactively accounting for uncertainties from both the supply and demand sides. To achieve that, an inclusive reward function was designed to incorporate market profits, carbon emissions, peak load management, and battery degradation. Two data-driven control schemes, i.e. prediction-based (PB) and prediction-free (PF), were adopted based on different problem formulations under the proposed D3QN architecture for the optimization of battery charging and discharging behaviours. The findings from extensive simulations not only validated the effectiveness of the proposed approach but also offered valuable guidance for its practical implementations. The contributions of this research can significantly advance the development of sustainable and resilient microgrid systems with high renewable penetration both onsite and from the grid. In the future work, we will implement the proposed approach on microgrid systems integrated with multiple RES (e.g. photovoltaic, wind) and ESS (e.g. battery and thermal storage) to maximise its potential in bringing clean and affordable energy.

## ACKNOWLEDGMENT

Fulong Yao acknowledges the financial support of China Scholarship Council and Newcastle University for his PhD study. This work was supported in part by Royal Society and NSFC under grants IEC\NSFC\201107 and 62111530154.

## REFERENCES

- [1] Zhou, Y., Zhai, Q., & Wu, L. (2022). Optimal operation of regional microgrids with renewable and energy storage: Solution robustness and nonanticipativity against uncertainties. *IEEE Transactions on Smart Grid*, 13(6), 4218-4230.
- [2] Pinciroli, L., Baraldi, P., Compare, M., & Zio, E. (2023). Optimal operation and maintenance of energy storage systems in grid-connected microgrids by deep reinforcement learning. *Applied Energy*, 352, 121947.
- [3] Chen, T., & Bu, S. (2019, September). Realistic peer-to-peer energy trading model for microgrids using deep reinforcement learning. In *2019 IEEE PES Innovative Smart Grid Technologies Europe (ISGT-Europe)* (pp. 1-5). IEEE.
- [4] Sami, M. S., Abrar, M., Akram, R., Hussain, M. M., Nazir, M. H., Khan, M. S., & Raza, S. (2021). Energy management of microgrids for smart cities: A review. *Energies*, 14(18), 5976.
- [5] García-Triviño, P., Sarrias-Mena, R., García-Vázquez, C. A., Leva, S., & Fernández-Ramírez, L. M. (2023). Optimal online battery power control of grid-connected energy-stored quasi-impedance source inverter with PV system. *Applied Energy*, 329, 120286.
- [6] Zhao, X., Zhang, Y., Cui, X., Wan, L., Qiu, J., Shang, E., ... & Zhao, H. (2023). Wavelet Packet-Fuzzy Optimization Control Strategy of Hybrid Energy Storage Considering Charge-Discharge Time Sequence. *Sustainability*, 15(13), 10412.
- [7] Das, A., & Ni, Z. (2017). A computationally efficient optimization approach for battery systems in islanded microgrid. *IEEE Transactions on Smart Grid*, 9(6), 6489-6499.
- [8] Morstyn, T., Hredzak, B., Aguilera, R. P., & Agelidis, V. G. (2017). Model predictive control for distributed microgrid battery energy storage systems. *IEEE Transactions on Control Systems Technology*, 26(3), 1107-1114.
- [9] Sachs, J., & Sawodny, O. (2016). A two-stage model predictive control strategy for economic diesel-PV-battery island microgrid operation in rural areas. *IEEE Transactions on Sustainable Energy*, 7(3), 903-913.
- [10] Qiu, D., Wang, Y., Hua, W., & Strbac, G. (2023). Reinforcement learning for electric vehicle applications in power systems: A critical review. *Renewable and Sustainable Energy Reviews*, 173, 113052.
- [11] Ojand, K., & Dagdougui, H. (2021). Q-learning-based model predictive control for energy management in residential aggregator. *IEEE Transactions on Automation Science and Engineering*, 19(1), 70-81.
- [12] She, B., Li, F., Cui, H., Zhang, J., & Bo, R. (2022). Fusion of microgrid control with model-free reinforcement learning: review and vision. *IEEE Transactions on Smart Grid*.
- [13] Alabdullah, M. H., & Abido, M. A. (2022). Microgrid energy management using deep Q-network reinforcement learning. *Alexandria Engineering Journal*, 61(11), 9069-9078.
- [14] Yu, Y., Cai, Z., & Liu, Y. (2021). Double deep Q-learning coordinated control of hybrid energy storage system in island micro-grid. *International Journal of Energy Research*, 45(2), 3315-3326.
- [15] Cao, J., Harrold, D., Fan, Z., Morstyn, T., Healey, D., & Li, K. (2020). Deep reinforcement learning-based energy storage arbitrage with accurate lithium-ion battery degradation model. *IEEE Transactions on Smart Grid*, 11(5), 4513-4521.
- [16] Ji, Y., Wang, J., Xu, J., & Li, D. (2021). Data-driven online energy scheduling of a microgrid based on deep reinforcement learning. *Energies*, 14(8), 2120.
- [17] Harrold, D. J., Cao, J., & Fan, Z. (2022). Renewable energy integration and microgrid energy trading using multi-agent deep reinforcement learning. *Applied Energy*, 318, 119151.
- [18] Anderson, W. C. (2016). How Microgrid is Changing the Energy Landscape. *Energy Engineering*, 113(6), 53-62.
- [19] Rangel, N., Li, H., & Aristidou, P. (2023). An optimization tool for minimising fuel consumption, costs and emissions from Diesel-PV-Battery hybrid microgrids. *Applied Energy*, 335, 120748.
- [20] Zhang, Z., Du, J., Fedorovich, K. S., Li, M., Guo, J., & Xu, Z. (2022). Optimization strategy for power sharing and low-carbon operation of multi-microgrid IES based on asymmetric nash bargaining. *Energy Strategy Reviews*, 44, 100981.
- [21] Wang, D., Liu, Y., Li, B., Li, Y., Dai, Z., & Zhang, N. (2022, November). Low-carbon Optimal Scheduling for Microgrid Considering the Multi-energy Cloud Energy Storage. In *2022 IEEE 6th Conference on Energy Internet and Energy System Integration (EI2)* (pp. 2987-2993). IEEE.
- [22] Ku, T. T., & Li, C. S. (2021). Implementation of battery energy storage system for an island microgrid with high PV penetration. *IEEE Transactions on Industry Applications*, 57(4), 3416-3424.
- [23] Kaelbling, L. P., Littman, M. L., & Moore, A. W. (1996). Reinforcement learning: A survey. *Journal of artificial intelligence research*, 4, 237-285.
- [24] Mnih, V., Kavukcuoglu, K., Silver, D., Rusu, A. A., Veness, J., Bellemare, M. G., ... & Hassabis, D. (2015). Human-level control through deep reinforcement learning. *nature*, 518(7540), 529-533.
- [25] Watkins, C. J. C. H. (1989). Learning from delayed rewards.
- [26] Sewak, M., & Sewak, M. (2019). Deep Q Network (DQN), Double DQN, and Dueling DQN: A Step Towards General

- Artificial Intelligence. *Deep Reinforcement Learning: Frontiers of Artificial Intelligence*, 95-108.
- [27] Sutton, R. S., & Barto, A. G. (2018). Reinforcement learning: An introduction. *MIT press*.
- [28] Sutton, R. S. (1988). Learning to predict by the methods of temporal differences. *Machine learning*, 3(1), 9–44.
- [29] Kim, J., & Yang, I. (2020, July). Hamilton-Jacobi-Bellman equations for Q-learning in continuous time. In *Learning for Dynamics and Control* (pp. 739-748). PMLR.
- [30] Xiao, H., Pu, X., Pei, W., Ma, L., & Ma, T. (2023). A novel energy management method for networked multi-energy microgrids based on improved DQN. *IEEE Transactions on Smart Grid*.
- [31] Amari, S. I. (1993). Backpropagation and stochastic gradient descent method. *Neurocomputing*, 5(4-5), 185-196.
- [32] Schaul, T., Quan, J., Antonoglou, I., & Silver, D. (2015). Prioritized experience replay. *arXiv preprint arXiv:1511.05952*.
- [33] Van Hasselt, H., Guez, A., & Silver, D. (2016, March). Deep reinforcement learning with double q-learning. In *Proceedings of the AAAI conference on artificial intelligence* (Vol. 30, No. 1).
- [34] Wang, Z., Schaul, T., Hessel, M., Hasselt, H., Lanctot, M., & Freitas, N. (2016, June). Dueling network architectures for deep reinforcement learning. In *International conference on machine learning* (pp. 1995-2003). PMLR.
- [35] Song, H., Liu, Y., Zhao, J., Liu, J., & Wu, G. (2021). Prioritized replay dueling DDQN based grid-edge control of community energy storage system. *IEEE Transactions on Smart Grid*, 12(6), 4950-4961.
- [36] Tokic, M. (2010, September). Adaptive  $\epsilon$ -greedy exploration in reinforcement learning based on value differences. In *Annual Conference on Artificial Intelligence* (pp. 203-210). Berlin, Heidelberg: Springer Berlin Heidelberg.
- [37] ChongAih. (2020, November). District dataset on Github. Retrieved Aug. 2023, from: <https://github.com/ChongAih/data>
- [38] WattTime. (n.d.). WattTime API. Retrieved Aug. 2023, from: <https://docs.watttime.org/>
- [39] FLYao123. (2023, July). District microgrid dataset on Github, Retrieved Aug. 2023, from: <https://github.com/FLYao123/District-microgrid-dataset>
- [40] Zhou, Y., Cao, S., & Hensen, J. L. (2021). An energy paradigm transition framework from negative towards positive district energy sharing networks—Battery cycling aging, advanced battery management strategies, flexible vehicles-to-buildings interactions, uncertainty and sensitivity analysis. *Applied Energy*, 288, 116606.
- [41] Ouyang, D., Chen, M., Liu, J., Wei, R., Weng, J., & Wang, J. (2018). Investigation of a commercial lithium-ion battery under overcharge/over-discharge failure conditions. *RSC advances*, 8(58), 33414-33424.
- [42] Amin, M. A., Suleman, A., Waseem, M., Iqbal, T., Aziz, S., Faiz, M. T., ... & Saleh, A. M. (2023). Renewable energy maximization for Pelagic Islands network of microgrids through battery swapping using deep reinforcement learning. *IEEE Access*.